Trabecular bone

- foam-like structure
- exists at ends of long bones - ends have larger surface area than shafts to reduce stress on cartilage at joints; trabecular bone reduces weight
- also exists in skull, iliac crest (pelvis) - forms sandwich structure - reduces wt.
- also makes up core of vertebrae
- trabecular bone of interest (1) osteoporosis (2) osteoarthritis (3) joint replacement

---

Osteoporosis

- bone mass decreases with age; osteoporosis - extreme bone loss
- Most common fractures: hip (proximal femur)
  vertebrae
- at both sites, most of load carried by trabecular bone
- hip fractures especially serious: 40% of elderly patients (>65 ys old) die within a year (often due to loss of mobility → pneumonia)
- 300,000 hip fractures/yr in US
- costs $17 billion in 2005

Trabecular bone

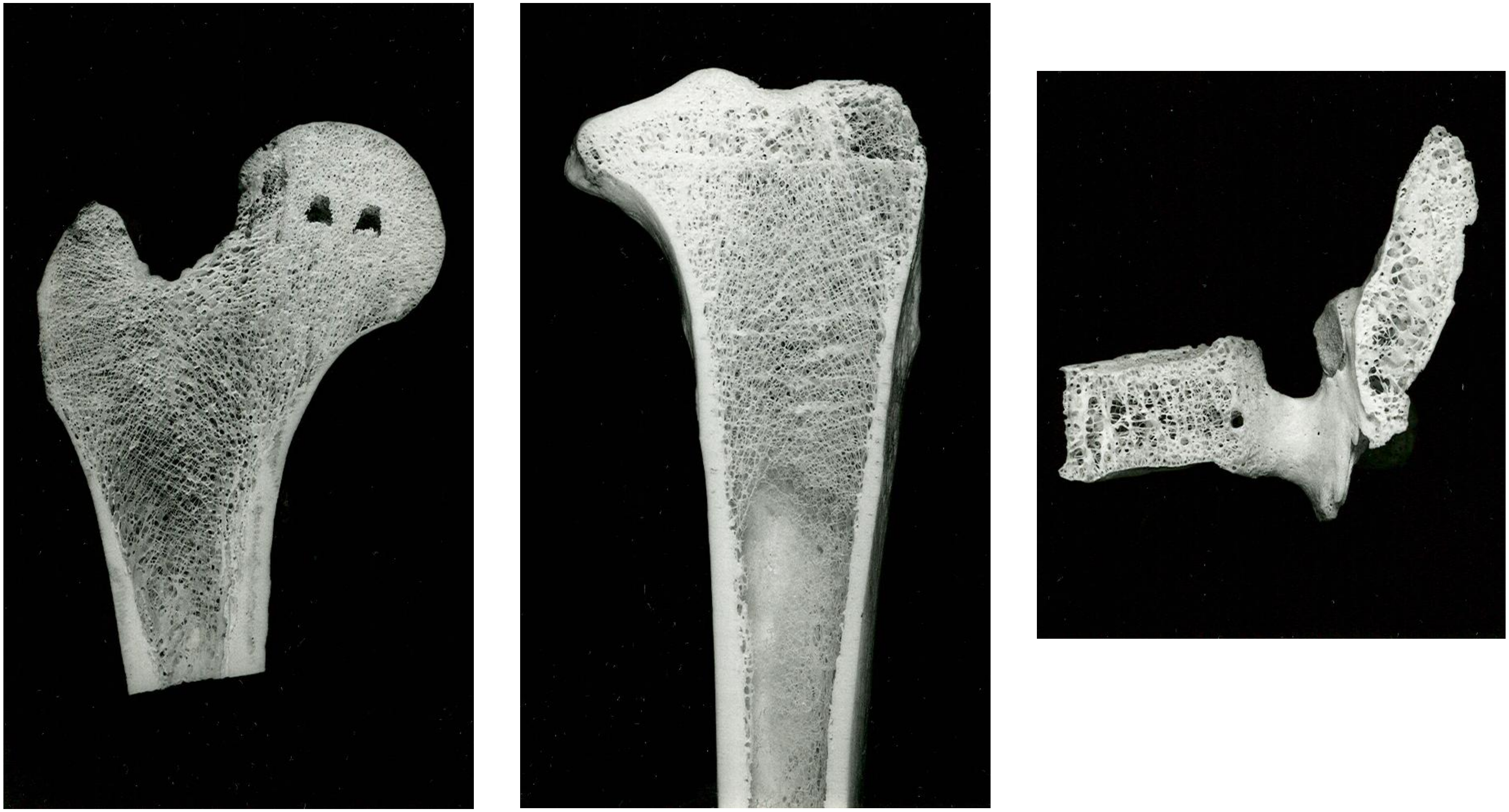

Gibson, L. J., and M. F. Ashby. *Cellular Solids: Structure and Properties*. 2nd ed. Cambridge University Press, © 1997. Figures courtesy of Lorna Gibson and Cambridge University Press.

Osteoarthritis

- degradation of cartilage at joints
- stress on cartilage affected by moduli of underlying bone
- cortical bone shell can be thin (e.g. <1 mm)
- mechanical properties of trabecular bone can affect stress distribution on cartilage

---

Joint replacements

- if osteoarthritis bad + significant damage to cartilage, may require joint replacement
- cut end of bone off + insert stem of metal replacement into hollow of long section of bone
- metals used: titanium, cobalt-chromium, stainless steel
- bone grows in response to loads on it

  trab. bone: density depends on magnitude of σ
  orientation " " direction of principal stresses

- mismatch in moduli between metal + bone leads to stress shielding

	E (GPa)		E (GPa)
Co - 28Cr · Mo	210	Cortical bone	18
Ti alloys	110	Trab. bone	0.01 - 2
316 Stainless steel	210		

- after joint replacement, remodelling of remaining bone affected
  - stiffer metal carries more of load, remaining bone carries less
  - bone may resorb - can lead to loosening of posthesis
  - can cause problems after ~ 15 yrs.
  - reason surgeons don't like to do joint replacements on younger patients

---

Structure of trabecular bone

- resembles foam : "trabecula" = little beam (latin)
- relative density typically 0.05 - 0.50
- low density trab. bone - like open cell foam
- higher density - becomes like perforated plates
- can be highly anisotropic, depending on stress field.

Trabecular Bone Structure

Images removed due to copyright restrictions.

Lumbar spine	Femoral head	Lumbar spine
11% dense	26% dense	6% dense
42 year old male	37 year old male	59 year old male

Ralph Muller, ETH Zurich
Micro-CT images

Trabecular Bone Structure

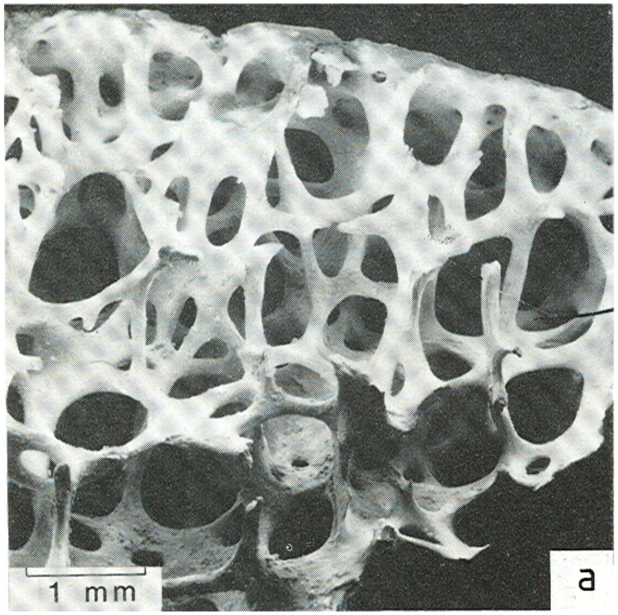

Femoral head

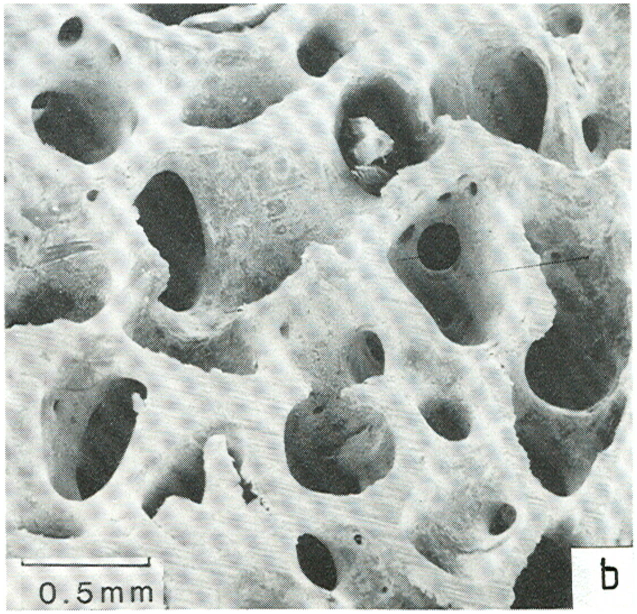

Femoral head

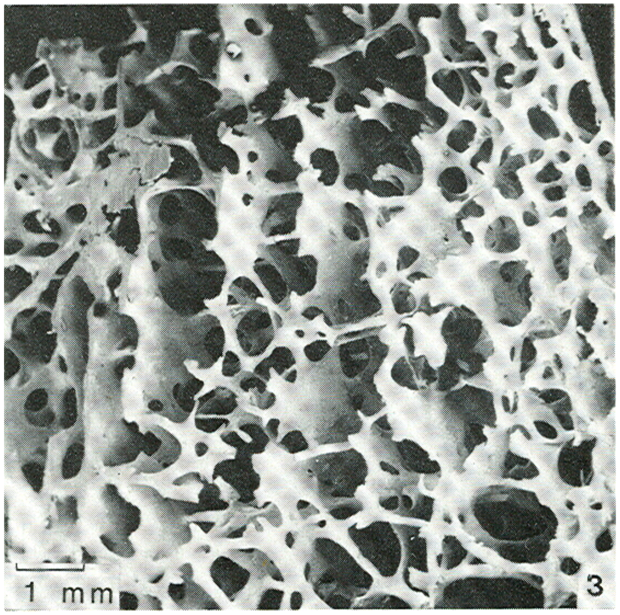

Femoral condyle (knee)

Source: Gibson. L. J. "The Mecahnical Behaviour of Cancellous Bone." *Journal of Biomechanics* 18 (1985): 317-28. Courtesy of Elsevier. Used with permission.

Bone grows in response to loads

- studies on juvenile guinea fowl (Ponzer et al. 2006)
  - (a) running on level treadmill
  - (b) " " inclined " (20°)
  - (c) control - no running.
- Measured knee flexion angle at max force on treadmill
- after ~6 wks, sacrificed birds + measured orientation of peak trabecular density (OPTD)

- knee flexion angle changed by 13.7° with incline vs. level treadmill running
- OPTD " " 13.6 " " " " "
- orientation of trabecula changed to match orientation of loading
- video: Concord Field station (Science Friday)

Trabecular architecture and mechanical loading

Figure removed due to copyright restrictions. See Figure 1: Pontzer, H., et al. "Trabecular Bone in the Bird Knee Responds with High Sensitivity to Changes in Load Orientation." *The Journal of Experimental Biology* 209 (2006): 57-65.

Trabecular architecture and mechanical loading

Figure removed due to copyright restrictions. See Figure 7: Pontzer, H., et al. "Trabecular Bone in the Bird Knee Responds with High Sensitivity to Changes in Load Orientation." *The Journal of Experimental Biology* 209 (2006): 57-65.

Video: "Studying Locomotion With Rat Treadmills, Wind Tunnels." March 9, 2012. Science Friday. Accessed November 12, 2014.

Properties of solid in trabeculae

- foam models: require ρ_s, E_s σ_{ys} for the solid
- ultrasonic wave propagation $E_s = 15-18$ GPa
- finite element models of exact trabecular architecture from micro-CT scans
  if do uniaxial compression test - can measure E^* + back calculate E_s
  $E_s = 18$ GPa
- find properties of trabeculae (solid) similar to cortical bone

---

$\rho_s = 1800$ kg/m^3

$E_s = 18$ GPa

$\sigma_{ys} = 182$ MPa (comp)

$\sigma_{ys} = 115$ MPa (tension)

Mechanical Properties of Trabecular Bone

- compressive stress-strain curve - characteristic shape
- mechanisms of deformation + failure
  - usually bending followed by inelastic buckling
  - Sometimes, if trabeculae are aligned or very dense: axial def^n
  - observations by deformation stage in μCT; also FEA modelling
- tensile σ-ϵ curve: failure at smaller strains; trabecular microcracking

---

- data for E^* σ_c^* σ_T^* (normalized by values for cortical bone)
  - spread is large - anisotropy, alignment of trabecular orientation + loading direction, variations in solid properties, $\dot{\epsilon}$, species
- models - based on open-cell foams

comp. $E^*/E_s \propto (\rho^*/\rho_s)^2$ bending

$\sigma_{el}^*/E_s \propto (\rho^*/\rho_s)^2$ buckling

tension $\sigma_T^*/\sigma_{ys} \propto (\rho^*/\rho_s)^{3/2}$ plastic hinges

data generally consistent with models

also: statistical analysis of data

$E^*, \sigma_c^* \propto \rho^2$

note: comp: $\epsilon_{el}^* = \text{constant} = 0.7\%$

Compressive stress-strain curves

Figure removed due to copyright restrictions. See Fig. 1: Hayes, W. C., and D. R. Carter. "Postyield Behavior of Subchondral Trabecular Bone." *Journal of Biomedical Materials Research* 10, no. 4 (1976): 537-44.

Hayes and Carter, 1976

Compression
Whale Vertebra

Images removed due to copyright restrictions. See Figure 5: Müller, R. S. C. Gerber, and W. C. Hayes. "Micro-compression: A Novel Technique for the Non-destructive Assessment of Bone Failure." *Technology and Health Care* 6 (1998): 433-44.

Muller et al, 1998

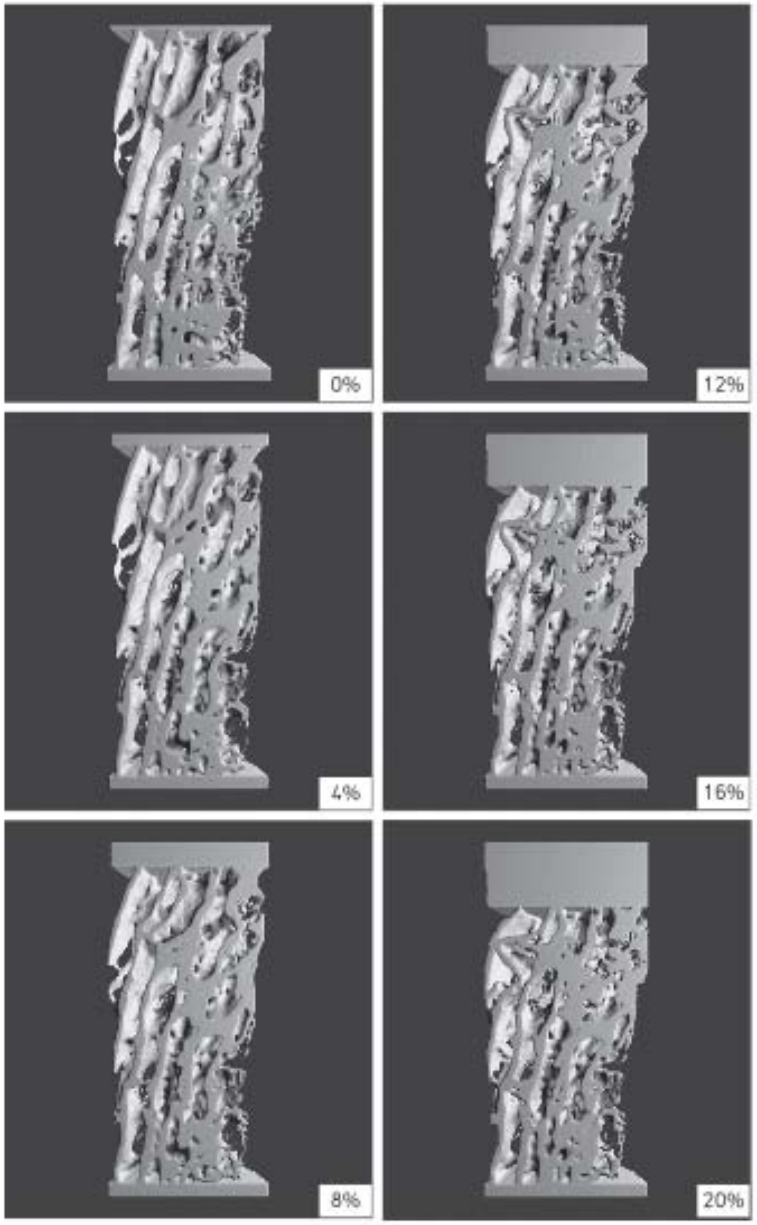

Nazarian and Muller 2004

Source: Narzarian, A., and R. Müller. "Time-lapsed Microstructural Imaging of Bone Failure Behavior." *Journal of Biomechanics* 37 (2000): 1575-83. Courtesy of Elsevier. Used with permission.

Images removed due to copyright restrictions.

Human Vertebral Bone

Mueller, ETH

Tension

Figure removed due to copyright restrictions. See Fig. 5.6: Gibson, L. J., et al. *Cellular Materials in Nature and Medicine*. Cambridge University Press, 2010.

Carter et al., 1980

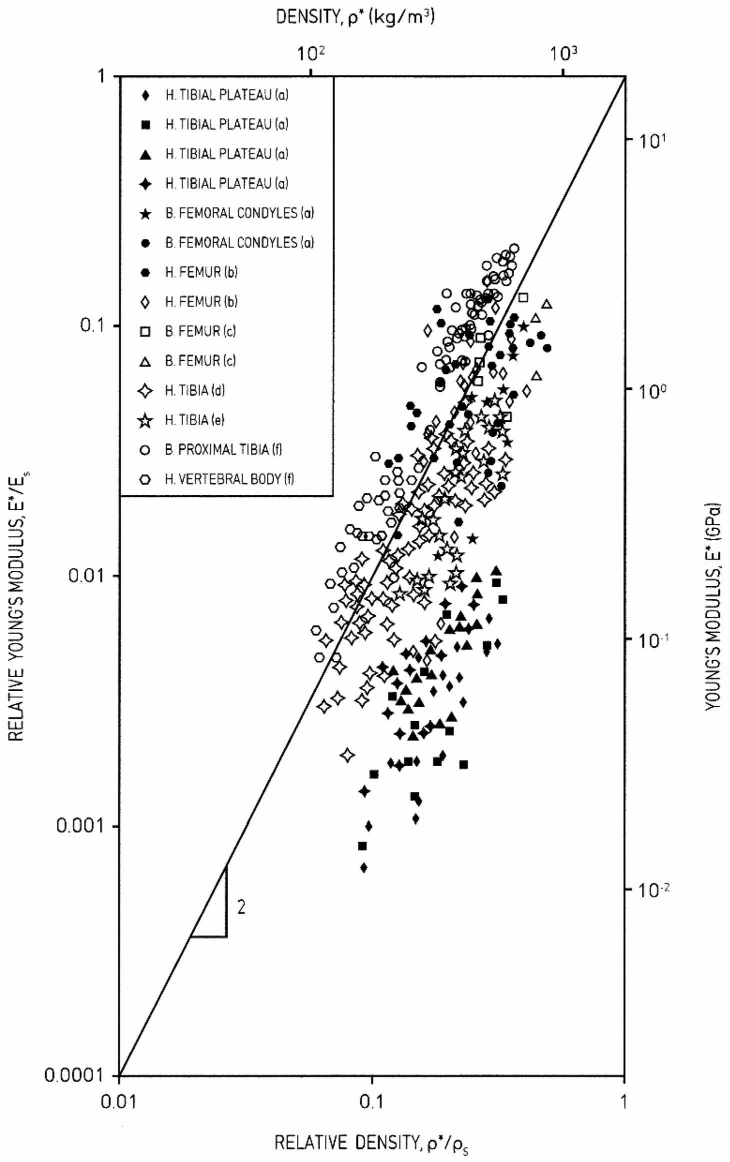

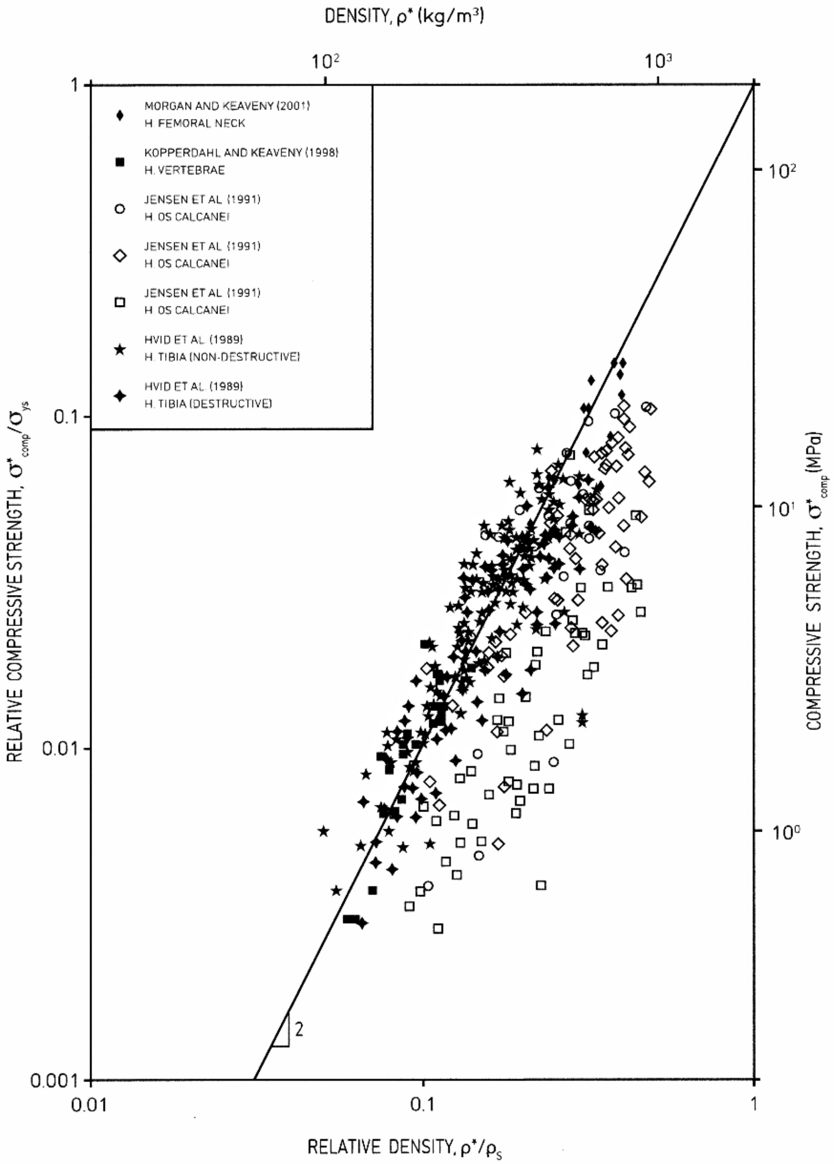

Gibson, L. J., M. Ashby, et al. *Cellular Materials in Nature and Medicine*. Cambridge University Press, © 2010. Figures courtesy of Lorna Gibson and Cambridge University Press.

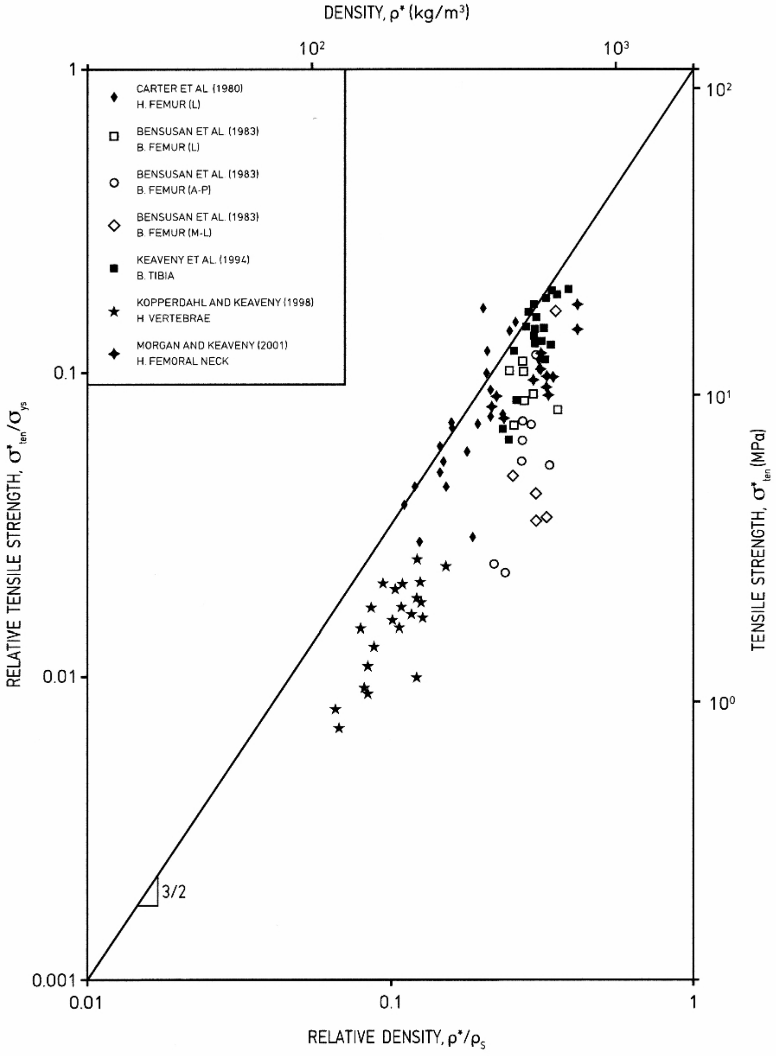

Gibson, L. J., M. Ashby, et al. *Cellular Materials in Nature and Medicine*. Cambridge University Press, © 2010. Figure courtesy of Lorna Gibson and Cambridge University Press.

- in some regions, trab. may be aligned e.g. parallel plates
  - deformation then axial (in longitudinal direction) $E^* \propto \rho$ $\sigma^* \propto \rho$

- can also summarize data for solid trabeculae + trabecular bone (similar to wood)

  solid - composite of hydroxyapatite + collagen

<u>Osteoporosis</u> (Latin "porous bones"

- as age, lose bone mass
- bone mass peaks at 25yrs, then decreases 1-2%/yr.
- women, menopause - cessation of estrogen production, increases rate of bone loss
- osteoporosis defined as bone mass 2.5 standard deviations (or more) below young normal mean
- trabeculae thin & then resorb completely

Aligned Trabeculae

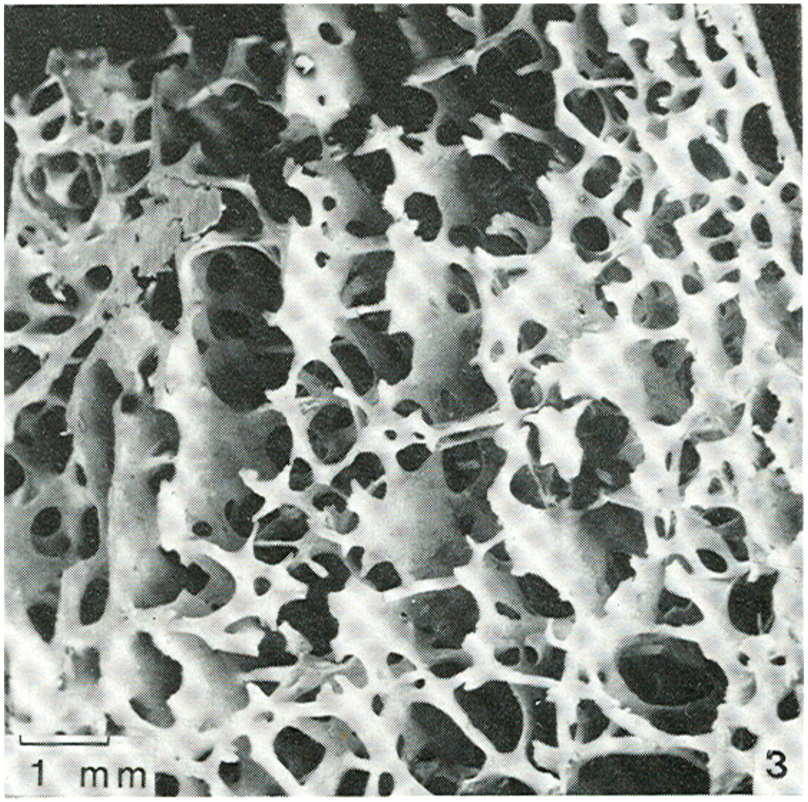

Femoral Condyle (Knee)

Source: Gibson. L. J. "The Mecahnical Behaviour of Cancellous Bone." *Journal of Biomechanics* 18 (1985): 317-28. Courtesy of Elsevier. Used with permission.

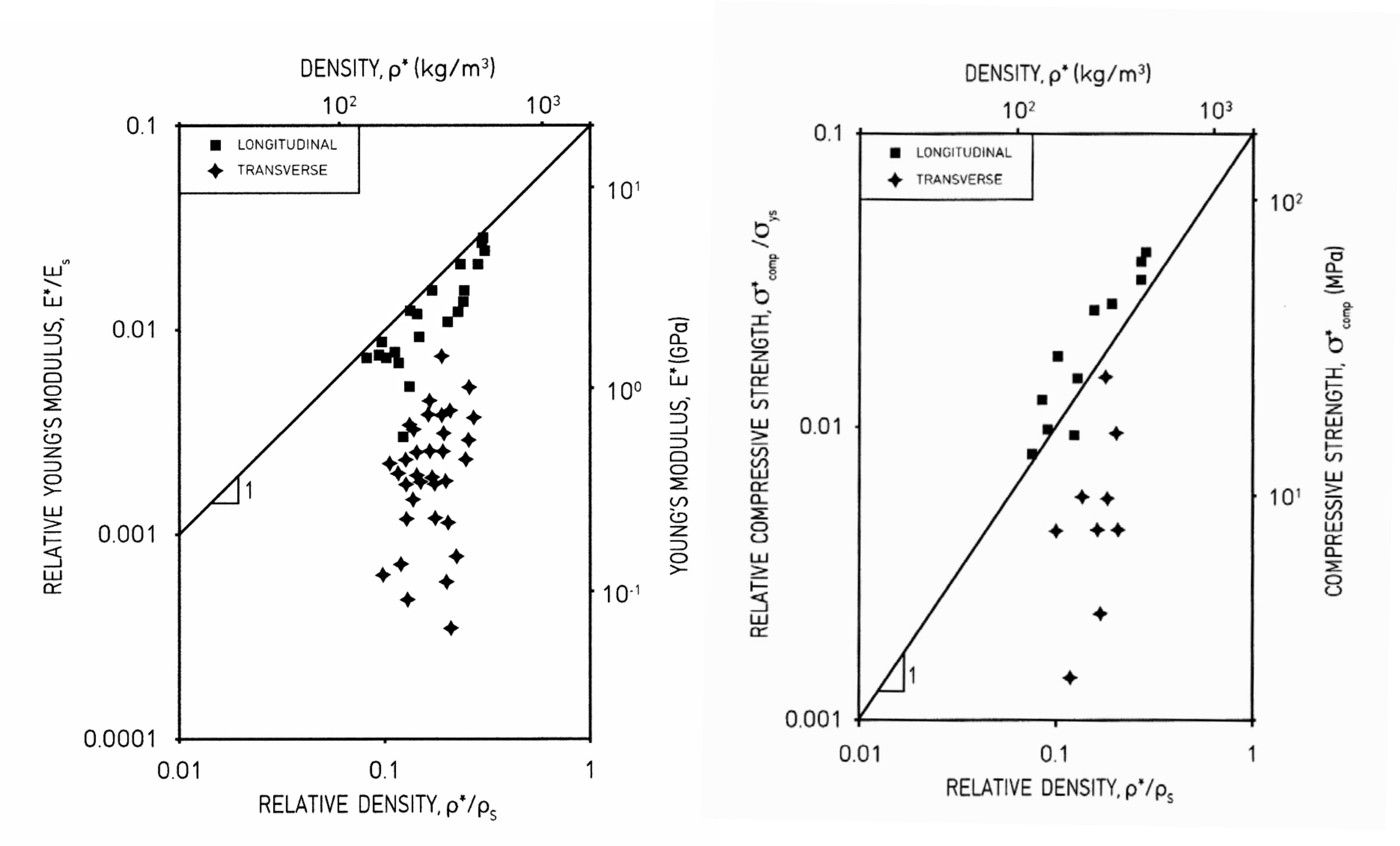

Gibson, L. J., M. Ashby, et al. *Cellular Materials in Nature and Medicine*. Cambridge University Press, © 2010. Figures courtesy of Lorna Gibson and Cambridge University Press.

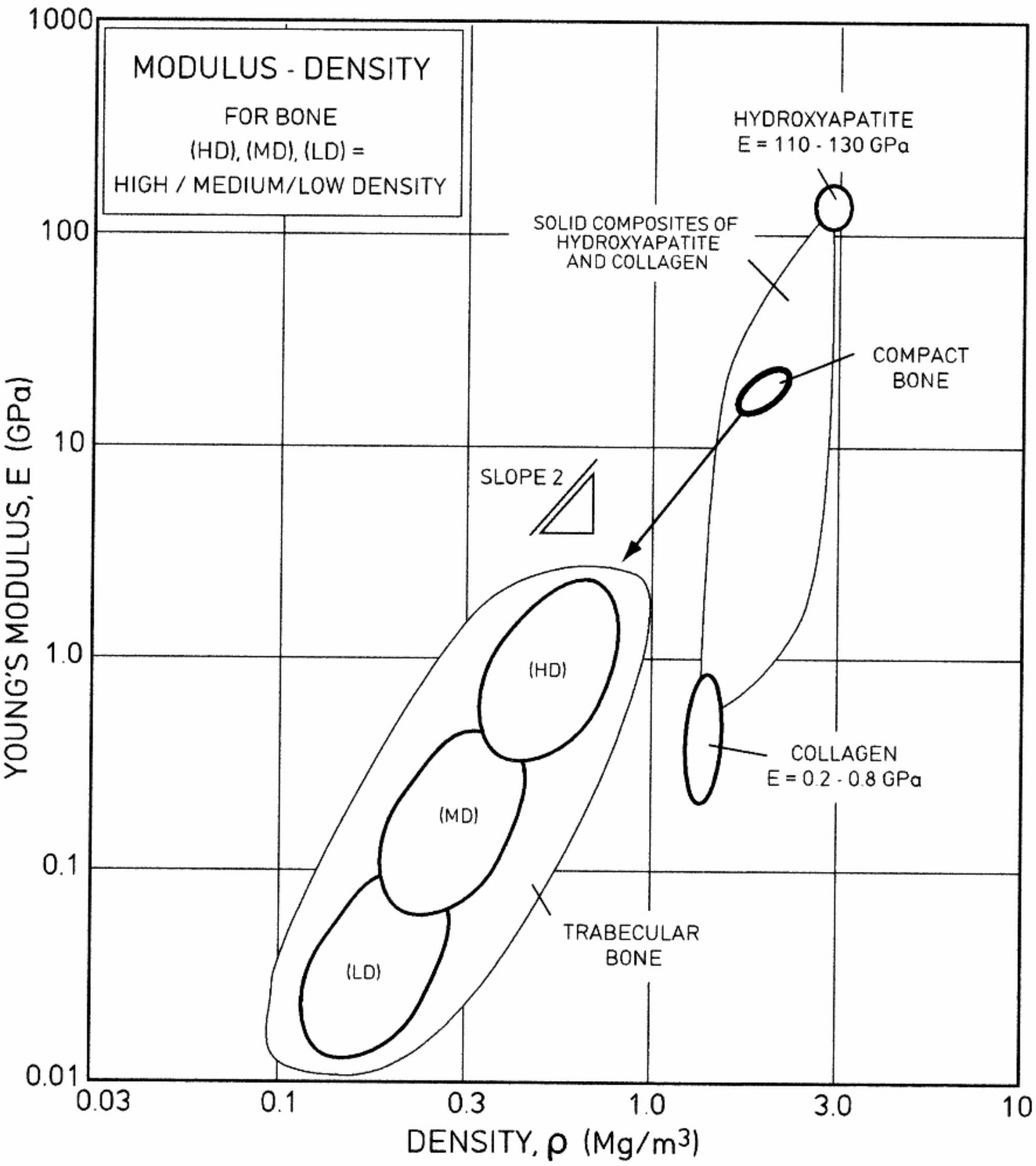

Gibson, L. J., M. Ashby, et al. *Cellular Materials in Nature and Medicine*. Cambridge University Press, © 2010. Figure courtesy of Lorna Gibson and Cambridge University Press.

Osteoporosis

Figure removed due to copyright restrictions. See Figure 1: Vajjhala, S., A. M. Kraynik, et al. "A Cellular Solid Model for Modulus Reduction due to Resorption of Trabecular Bone." *Journal of Biomechanical Engineering* 122, no. 5 (2000): 511–15.

- as trabeculae thin - buckling easier $\sigma^* \propto (\rho/\rho_s)^2$
- once trabeculae begin to resorb, connectivity reduced, strength drops dramatically
- Modelling
  - can't use unit cell or dimensional analysis (need to model local effects)
  - finite element modelling
  - initially - 2D Voronoi honeycomb
    - 2D representation of vertebral bone] Matt Silva
    - 3D Voronoi foam - Suretha Vajjhala

Voronoi honeycomb

- random seed points, draw perpendicular bisectors
- use a minimum separation distance to get cells of approximately uniform size
- FE analysis - each trabecula a beam element
- first calculated elastic moduli
  - FEA results close to analytical model for random (isotropic) honeycomb (40 models, all same ρ^*/ρ_s, about 25x25 cells in each)
  - modulus is average of stiffness over entire material

Modelling: 2D Voronoi

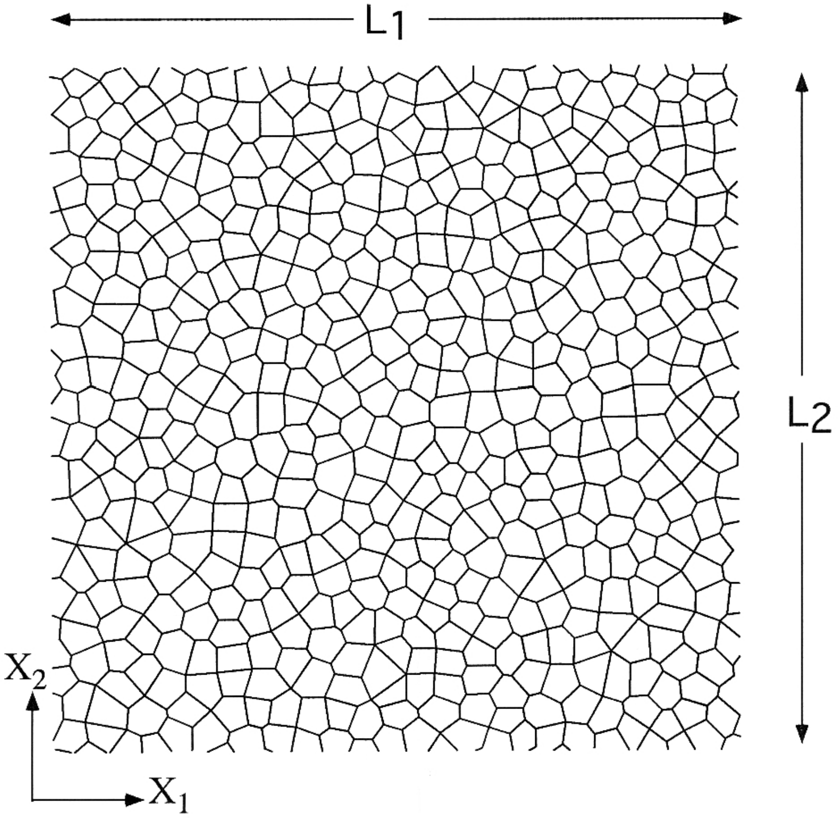

Silva et al, 1995

Source: Silva, M. J., L. J. Gibston, et al. "The Effects of Non-periodic Microstructure on the Elastic Properties of Two-dimensional Cellular Solids." *International Journal of Mechanical Sciences* 37 (1995): 1161-77. Courtesy of Elsevier. Used with permission.

2D Voronoi

E^*/E_s	FEA	$y=0.56x^{2.43}$
E^*/E_s	Equation (1a)	$y=0.63x^{2.54}$
G^*/E_s	FEA	$y=0.18x^{2.53}$
G^*/E_s	Equation (3d)	$y=0.20x^{2.68}$
ν^*	FEA	$y= -1.20x^{1.38} + 1.0$
ν^*	Equation (1b)	$y= -1.30x^{1.55} + 1.0$

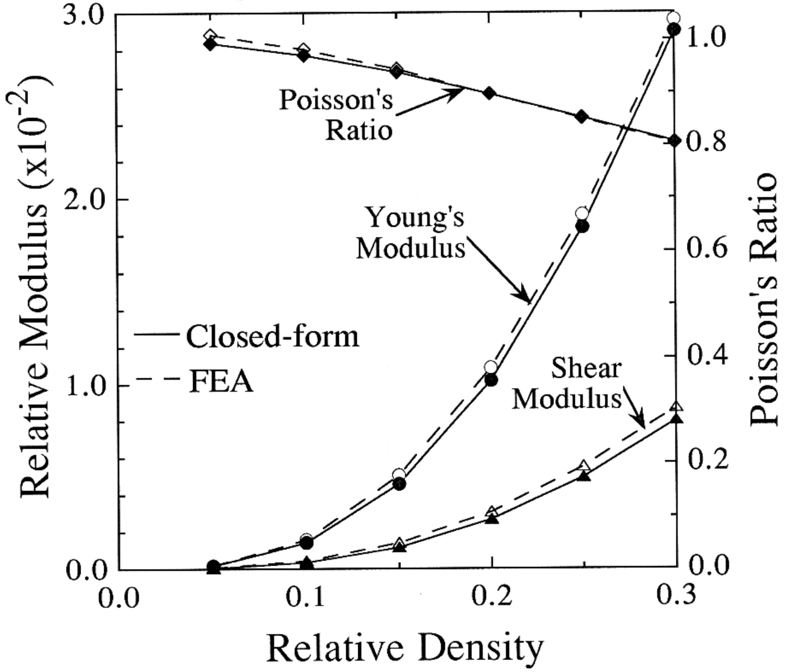

Silva et al, 1995

Source: Silva, M. J., L. J. Gibston, et al. "The Effects of Non-periodic Microstructure on the Elastic Properties of Two-dimensional Cellular Solids." *International Journal of Mechanical Sciences* 37 (1995): 1161-77. Courtesy of Elsevier. Used with permission.

- next, calculated compressive strength of Voronoi honeycombs
- each cell wall 1-3 beam elements
- model non-linear elasticity + failure behaviour
- 15 x 15 cells in model (random seeds ≈ isotropic)
- cell wall assumed to be elastic-perfectly plastic $\sigma_{ys}/E_s = 0.01$ $\nu = 0.3$
- for this value of σ_{ys}/E_s, transition between elastic buckling + plastic collapse stress at $\rho^*/\rho_s = 0.035$ in regular hex. honeycomb

---

- calculated compressive strength of honeycombs with $\rho^*/\rho_s = 0.015, 0.035, 0.05$ & 0.15
- generated 5 different Voronoi honeycombs at each ρ^*/ρ_s
- compressive σ-ϵ behaviour:

  $\rho^*/\rho_s \geq 0.05$ - strain softening, permanent def$^{\underline{n}}$ on unloading
  - plastic hinge formation, cell collapse in narrow localized bands

  $\rho^*/\rho_s < 0.035$ - non-linear elastic deformation - recoverable

  strength : 0.6 to 0.8 of $\sigma^*_{periodic}$

2D Voronoi

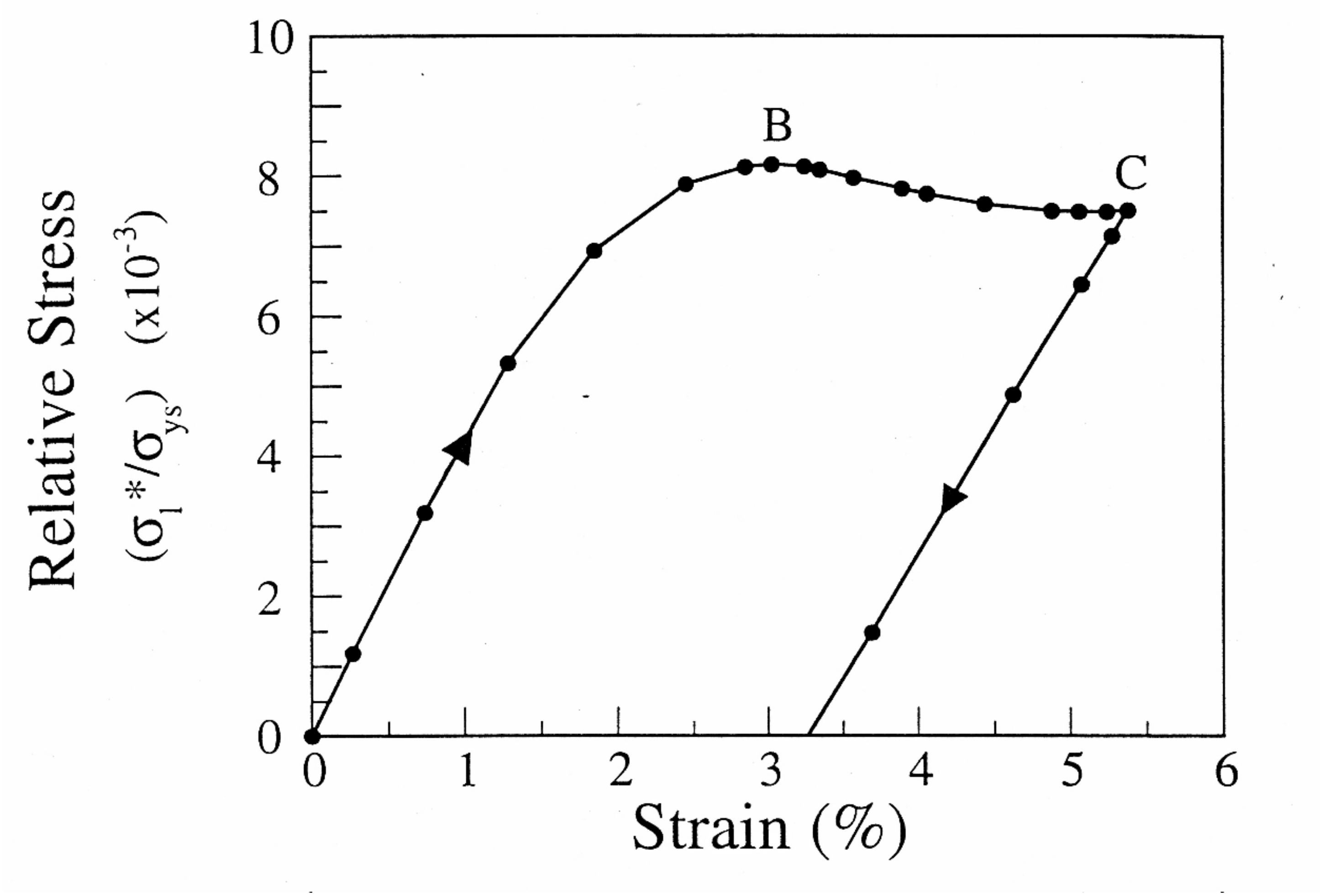

Relative density = 15% Plastic failure

Silva et al, 1997

Source: Silva, M. J., and L. J. Gibson. "The Effects of Non-periodic Microstructure and Defects on the Compressive Strength of Two-dimensional Cellular Solids." *International Journal of Mechanical Sciences* 39 (1997b): 549-63. Courtesy of Elsevier. Used with permission.

2D Voronoi

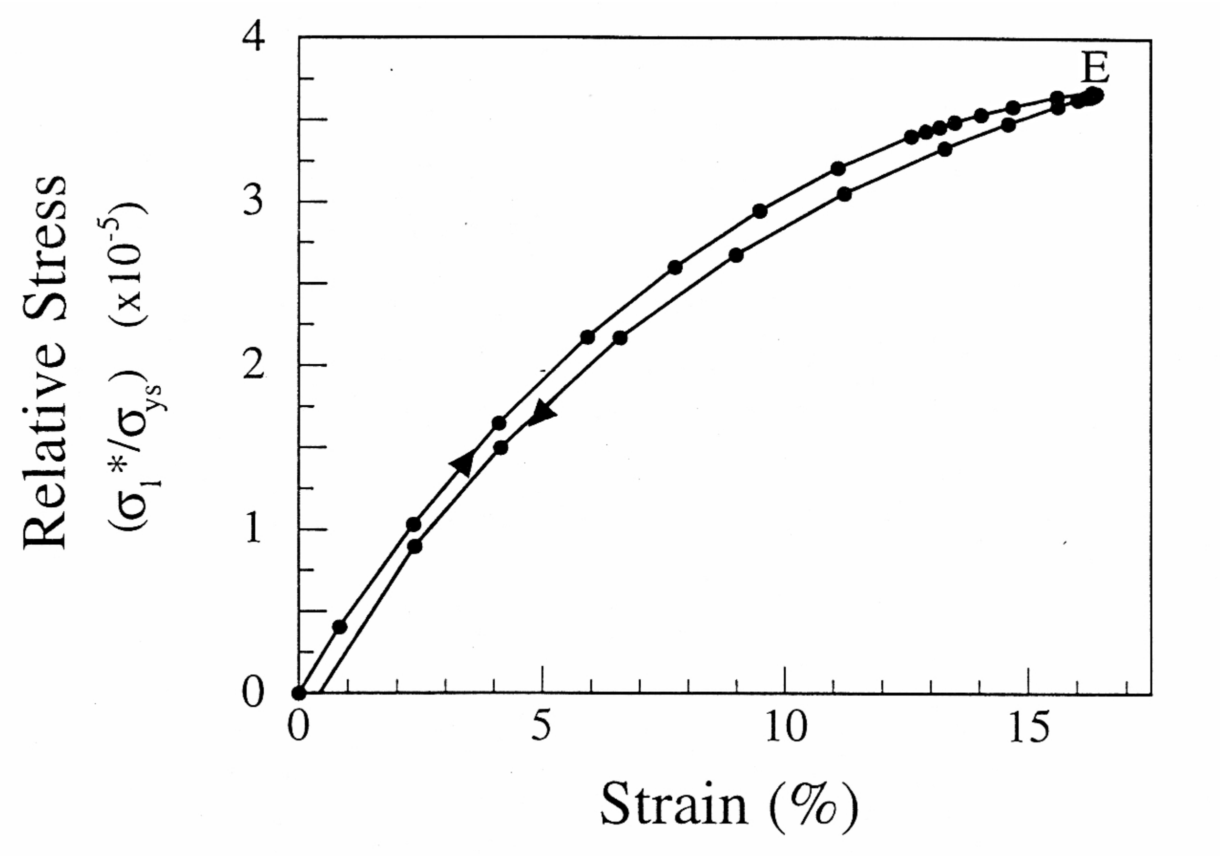

Relative density 1.5%; elastic buckling failure

Silva et al, 1997

Source: Silva, M. J., and L. J. Gibson. "The Effects of Non-periodic Microstructure and Defects on the Compressive Strength of Two-dimensional Cellular Solids." *International Journal of Mechanical Sciences* 39 (1997b): 549-63. Courtesy of Elsevier. Used with permission.

2D Voronoi

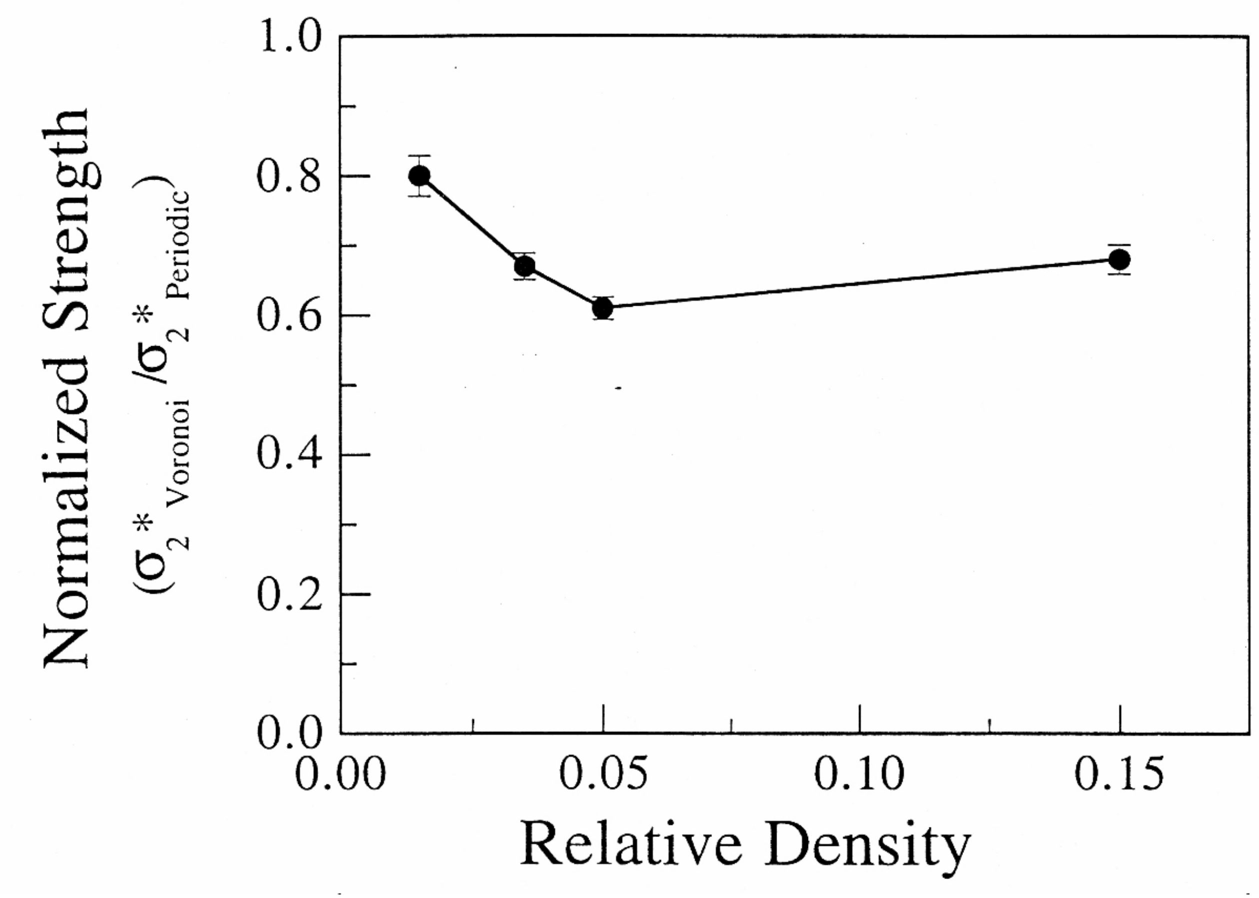

Silva et al, 1997

Source: Silva, M. J., and L. J. Gibson. "The Effects of Non-periodic Microstructure and Defects on the Compressive Strength of Two-dimensional Cellular Solids." *International Journal of Mechanical Sciences* 39 (1997b): 549-63. Courtesy of Elsevier. Used with permission.

- max. normal strains at nodes in honeycombs (linear elastic)
  - Voronoi honeycombs - normal distribution
  - regular hexagonal honeycombs - dashed lines on plot
  - normal strain in vertical cell walls in regular hex. honeycomb ≈ mean normal strain in Voronoi
  - oblique walls - bending - larger strains
  - Voronoi honeycomb 5% of strains outside of range of strain in regular hex. honeycomb

---

- decrease in strength associated with broader range of strains in Voronoi honeycombs
- minimum strength @ $\rho^*/\rho_s = 0.05$
  - interaction between elastic buckling + plastic yield

pin ended column

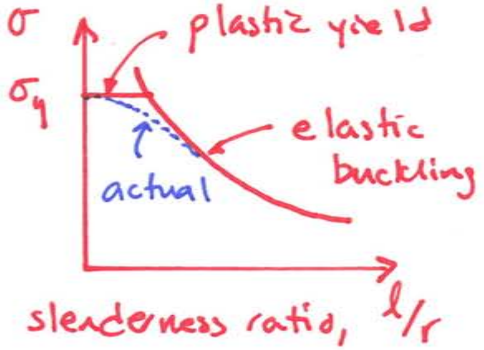

$$\sigma_{cr} = \frac{\pi^2 E I}{l^2} = \frac{\pi^2 E \, \pi r^4}{4 l^2 \, \pi r^2} = \frac{\pi^2}{4} E \left(\frac{r}{l}\right)^2$$

2D Voronoi

Figure removed due to copyright restrictions. See Figure 5; Silva, M. J., and L. J. Gibson. "The Effects of Non-periodic Microstructure and Defects on the Compressive Strength of Two-dimensional Cellular Solids." *International Journal Mechanical Sciences* 39, no. 5 (1997): 549-63.

Silva et al, 1997

Voronoi honeycombs - defects

- randomly removed cell walls in both Voronoi + reg. hex. honeycombs
- analyzed both by FEA
- dramatic decrease in modulus + strength, compared with equivalent reduction in density by thinning of cell walls
- $\rho^*/\rho_s = 0.15$ failure by yielding
- $\rho^*/\rho_s = 0.015$ " " elastic buckling

- Modulus + strength reduction similar for Voronoi + reg. hex. honeycombs
- percolation threshold for 2D network hexagonal cells ⇒ 35% struts removed

Vertebral trabecular bone - 2D model

- model adapted to reflect trabeculae more aligned in vertical + horizontal directions
- perturbed a square array of struts to get similar orientation of struts as in bone
- looked at reduction in number + thickness of longitudinal + transverse struts (independently)

2D Voronoi

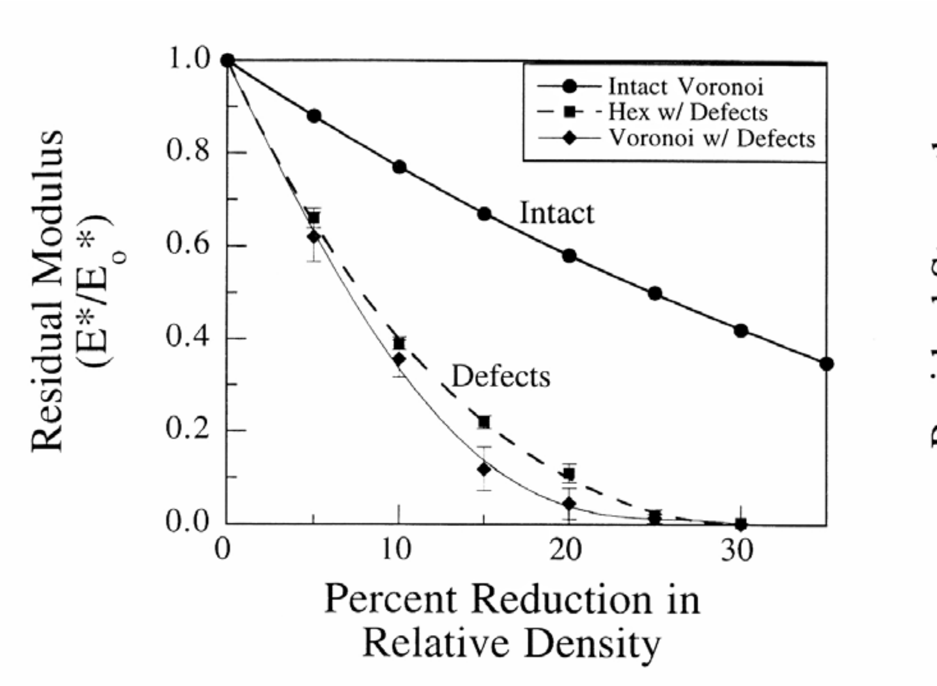

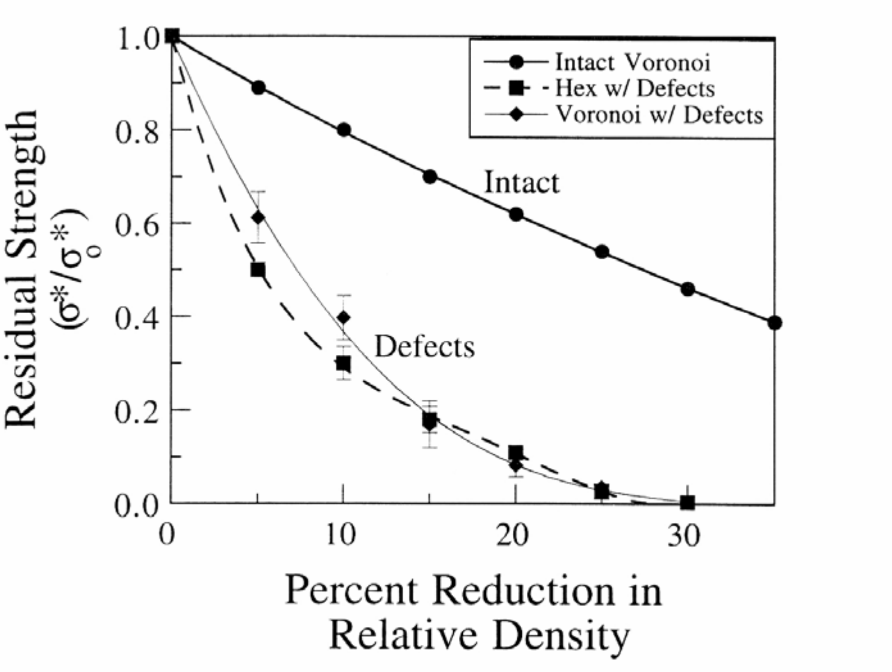

Source: Silva, M. J., and L. J. Gibson. "The Effects of Non-periodic Microstructure and Defects on the Compressive Strength of Two-dimensional Cellular Solids." *International Journal of Mechanical Sciences* 39 (1997b): 549-63. Courtesy of Elsevier. Used with permission.

Silva et al, 1997

2D Voronoi

Figure removed due to copyright restrictions. See Figure 2: Vajjhala, S., A. M. Kraynik, et al. "A Cellular Solid Model for Modulus Reduction due to Resorption of Trabecular Bone." *Journal of Biomechanical Engineering* 122, no. 5 (2000): 511–15.

Vajjhala et al, 2000

Vertebral Trabecular Bone

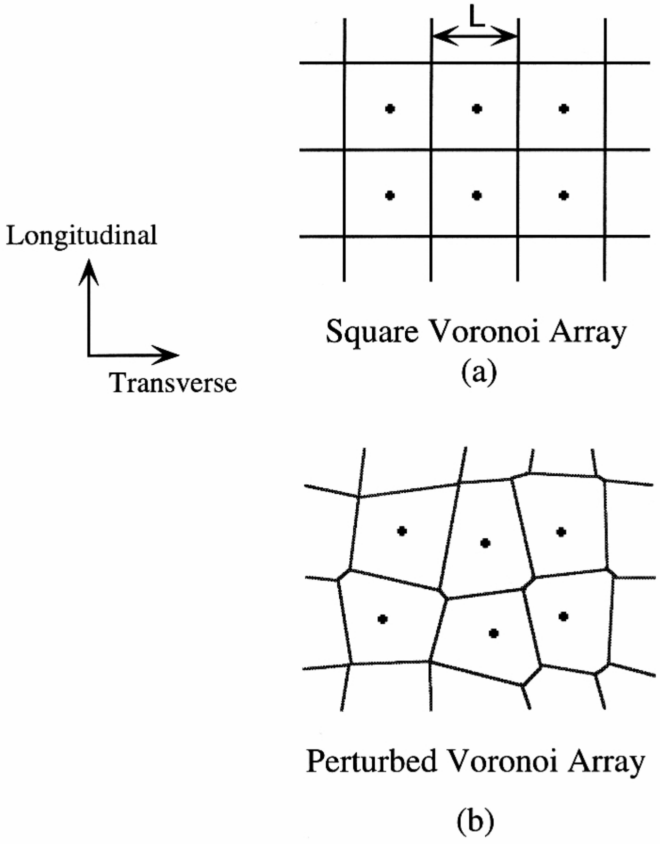

Source: Silva, M. J., and L. J. Gibson. "Modelling the Mechancial Behavior of Vertebral Trabecular Bone: Effects of Age-related Changes in Microstructure." *Bone* 21 (1997a): 191-99. Courtesy of Elsevier. Used with permission.

Silva et al, 1997

Vertebral Trabecular Bone

Figure removed due to copyright restrictions. See Figure 3: Silva, M. J., and L. J. Gibson. "Modelling the Mechancial Behavior of Vertebral Trabecular Bone: Effects of Age-related Changes in Microstructure." *Bone* 21 (1997): 191-99.

Silva et al, 1997

Vertebral Trabecular Bone

Figure removed due to copyright restrictions. See Figure 4: Silva, M. J., and L. J. Gibson. "Modelling the Mechancial Behavior of Vertebral Trabecular Bone: Effects of Age-related Changes in Microstructure." *Bone* 21 (1997): 191-99.

Silva et al, 1997

Vertebral Trabecular Bone

Figure removed due to copyright restrictions. See Figure 5: Silva, M. J., and L. J. Gibson. "Modelling the Mechancial Behavior of Vertebral Trabecular Bone: Effects of Age-related Changes in Microstructure." *Bone* 21 (1997): 191-99.

Silva et al, 1997

Vertebral Trabecular Bone

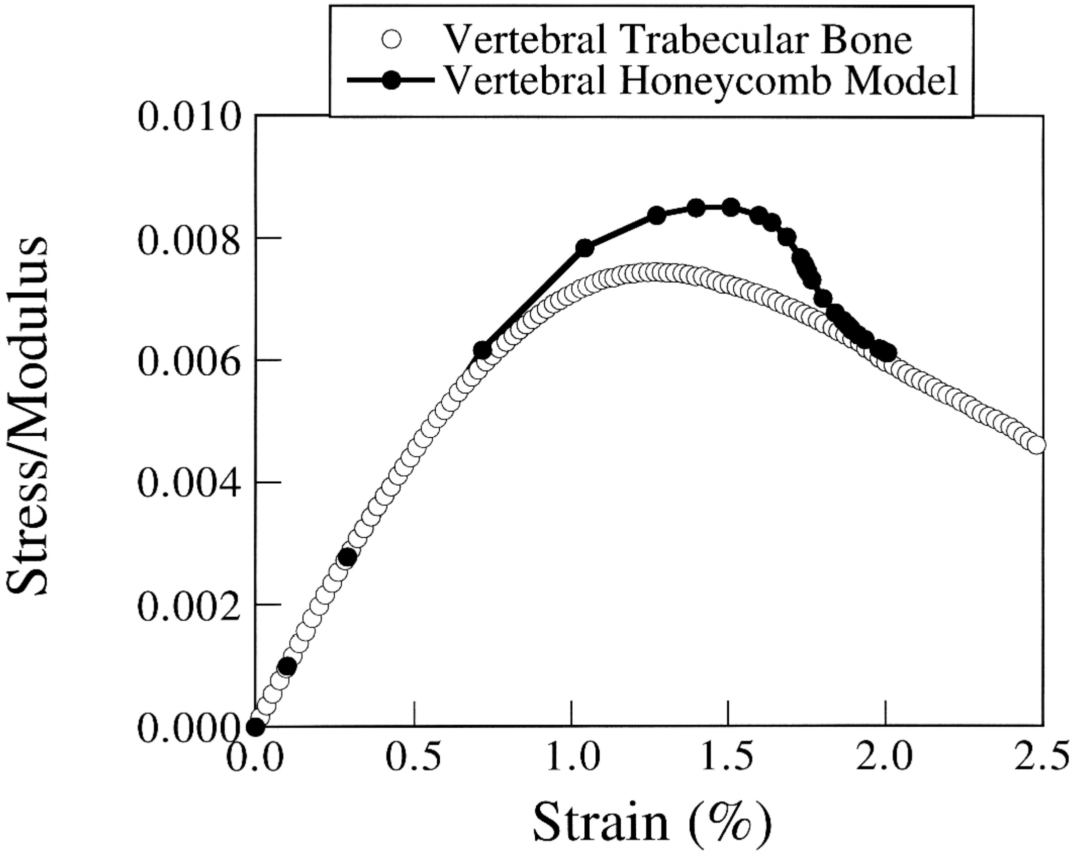

Source: Silva, M. J., and L. J. Gibson. "Modelling the Mechancial Behavior of Vertebral Trabecular Bone: Effects of Age-related Changes in Microstructure." *Bone* 21 (1997a): 191-99. Courtesy of Elsevier. Used with permission.

Silva et al, 1997

Vertebral Trabecular Bone

Figure removed due to copyright restrictions. See Figure 7: Silva, M. J., and L. J. Gibson. "Modelling the Mechancial Behavior of Vertebral Trabecular Bone: Effects of Age-related Changes in Microstructure." *Bone* 21 (1997): 191-99.

Silva et al, 1997

Vertebral Trabecular Bone

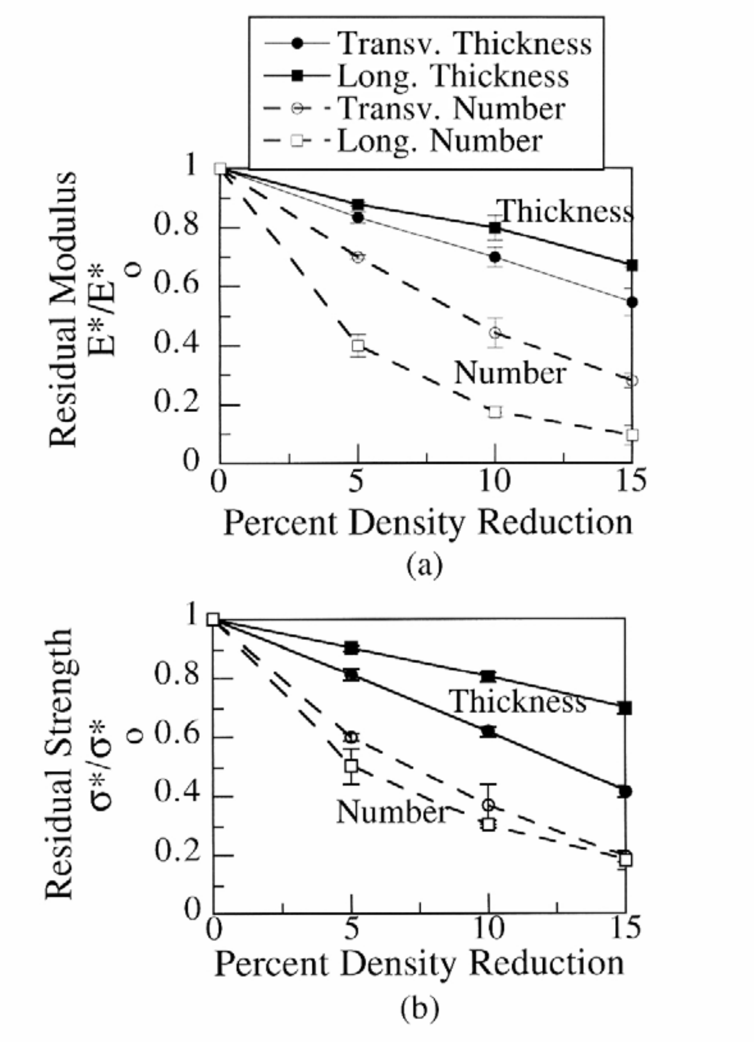

Silva et al, 1997

Source: Silva, M. J., and L. J. Gibson. "Modelling the Mechancial Behavior of Vertebral Trabecular Bone: Effects of Age-related Changes in Microstructure." *Bone* 21 (1997a): 191-99. Courtesy of Elsevier. Used with permission.

3D Voronoi Model

- same analysis, now with 3D Voronoi Model
- periodic 3×3×3 cells, $\rho^*/\rho_s = 0.1$
- used beam elements, FEA, linear elastic only
- percolation threshold ~ 50% struts removed
- comparison of 2D + 3D results for modulus: in 3D, modulus reduction more gradual than in 2D
- also for 2D + 3D - modulus reduction similar for regular + Voronoi structures

---

3D Voronoi Model

Figure removed due to copyright restrictions. See Figure 6: Vajjhala, S., A. M. Kraynik, et al. "A Cellular Solid Model for Modulus Reduction due to Resorption of Trabecular Bone." *Journal of Biomechanical Engineering* 122, no. 5 (2000): 511–15.

Vajjhala et al, 2000

3D Voronoi Model

Figure removed due to copyright restrictions. See Figure 7: Vajjhala, S., A. M. Kraynik, et al. "A Cellular Solid Model for Modulus Reduction due to Resorption of Trabecular Bone." *Journal of Biomechanical Engineering* 122, no. 5 (2000): 511–15.

Vajjhala et al, 2000

Metal foams as bone substitute materials

- metals used in orthopaedic implants (eg. hip, knee)
- Co-Cr, Ti, Ta, stainless steel alloys
- biocompatible, corrosion resistant
- but moduli of metals > modulus of bone

  e.g. $E_{Ti} = 110$ GPa $E_{cortical} = 18$ GPa $E_{trab.bone} = 0.01 - 2$ GPa
- stress shielding can lead to bone resorption.

- to improve mechanical interaction between implant + bone
  - porous sintered metal beads used to coat implants - promote bone ingrowth
  - also, wire mesh coatings have been developed, primarily for flat implant surfaces
  - recently, interest in using metal foams as coatings
  - longer term, interest in using in replacement vertebral bodies
- variety of processes for making metal foam implant coatings

Metal Foams: Microstructure

Ta, replicating PU foam with CVD

Ti, replication of PU foam by slurry infiltration and sintering

Ti, fugitive phase

Ti, foaming agent

Ti, expansion of Ar gas

Images removed due to copyright restrictions. See Figure 8.1: Gibson, L. J., M. Ashby, and B. A. Harley. *Cellular Materials in Nature and Medicine*. Cambridge University Press, 2010. http://books.google.com/books?id=AKxiS4AKpyEC&pg=PA228

Ti, freeze-casting (freeze-drying)

Ti, selective laser sintering

Ni-Ti, high temperature synthesis (powders mixed, pressed and ignited by, for example, tungsten coil heated by electrical current)

Image sources given in Cellular Materials in Nature and Medicine

Processing

(a) replicate open cell polyurethane foam

- pyrolize pu foam → 2% dense vitreous carbon
- coat with Ta by CVD ⇒ struts 99% Ta, 1% C
- cell size 400-600 μm; coating thickness 40-60 μm $\rho^*/\rho_s = 0.15-0.25$
- "Trabecular Metal" (Zimmer) trade name.
- Ta forms surface oxide Ta_2O_5 - does not bond to bone
- but, if treat with dilute NaOH, then heat to 300°C + cool, then submerge in simulated body fluid (ion conc. matches human blood plasma) ⇒ get apatite coating on foam struts, which bonds to bone

(b) infiltrate slurry of titanium hydride into open cell foam

- heat treat to decompose TiH_2
- sinter remaining Ti (also removes initial foam)

(c) fugitive phase methods

- mix Ti powder + fugitive phase powder
- heat to T_1 (~200°C) to decompose filler, then to T_2 (1200°C) to sinter Ti powder

Metal Foams: Processing

FUGITIVE FILLER

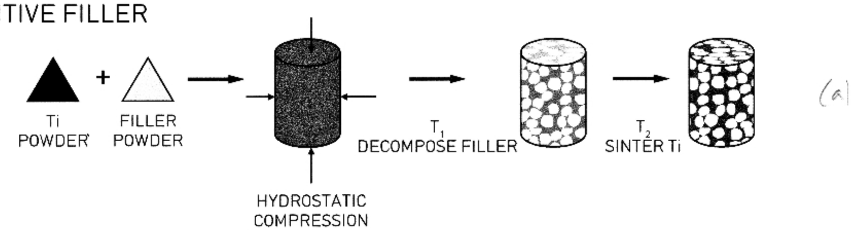

EXPANSION OF A FOAMING AGENT

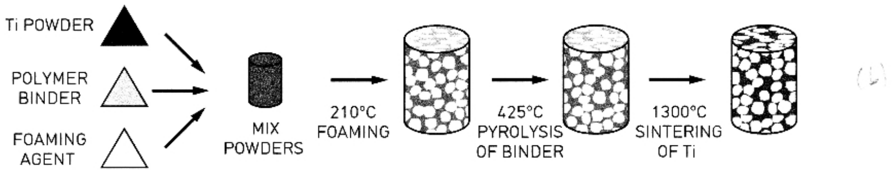

Foaming agent evolves gas at temperature at which polymer is liquid

FREEZE-CASTING

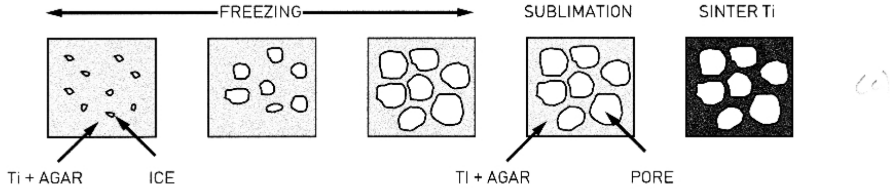

RAPID PROTOTYPING

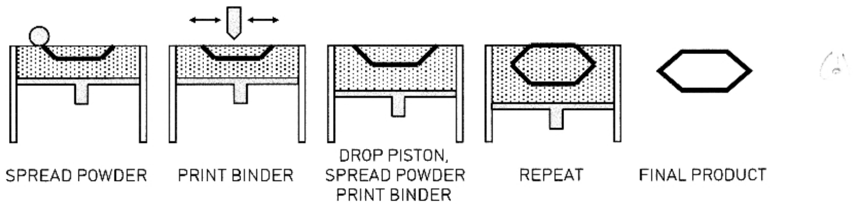

Gibson, L. J., M. Ashby, et al. *Cellular Materials in Nature and Medicine*. Cambridge University Press, © 2010. Figures courtesy of Lorna Gibson and Cambridge University Press.

Processes

(d) expansion of foaming agent

(e) freeze casting (freeze drying)

(f) rapid prototyping (3D Printing, selective laser sintering)

σ - ϵ curves - similar to other foams

data for E^*, σ_c^*

Ti Foam: Stress-strain

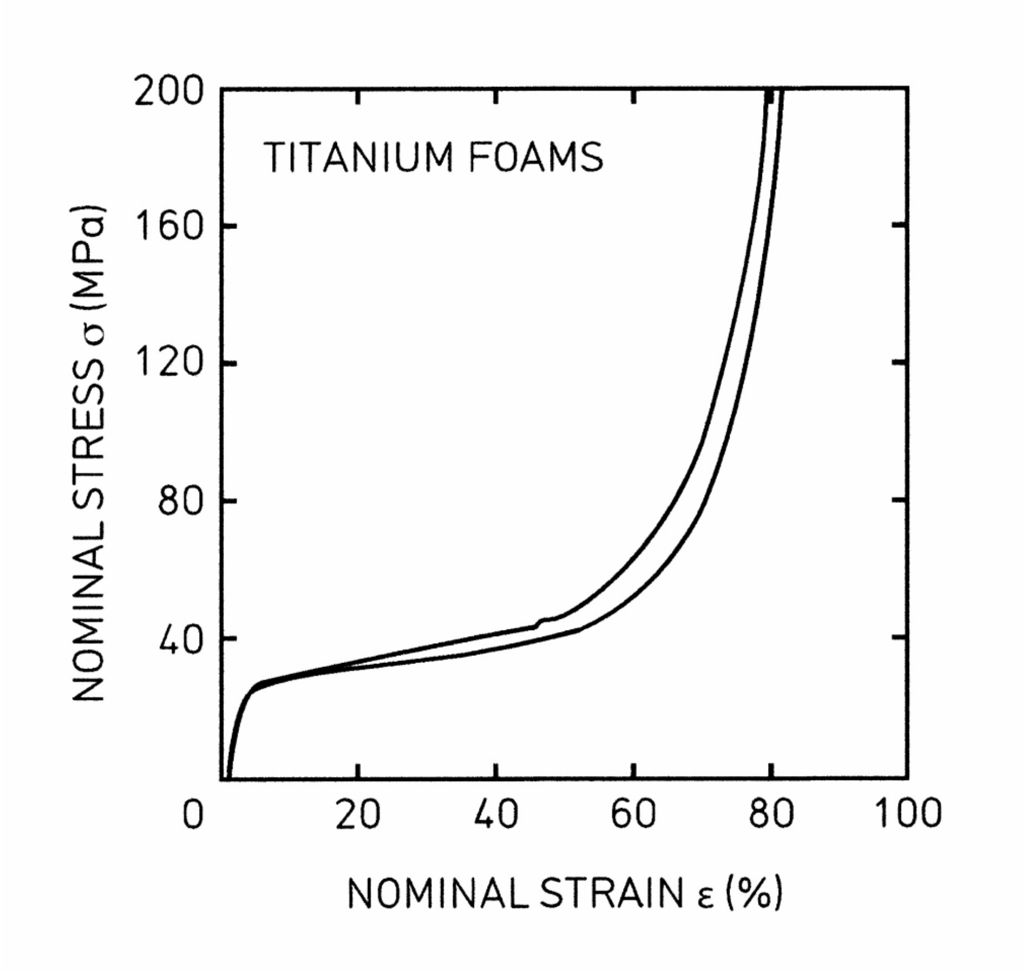

Source: Wen, C. E., M. Mabuchi, et al. "Processing of Biocompatible Porous Ti and Mg." *Scripta Materialia* 45 (2001): 1147-53. Courtesy of Elsevier. Used with permission.

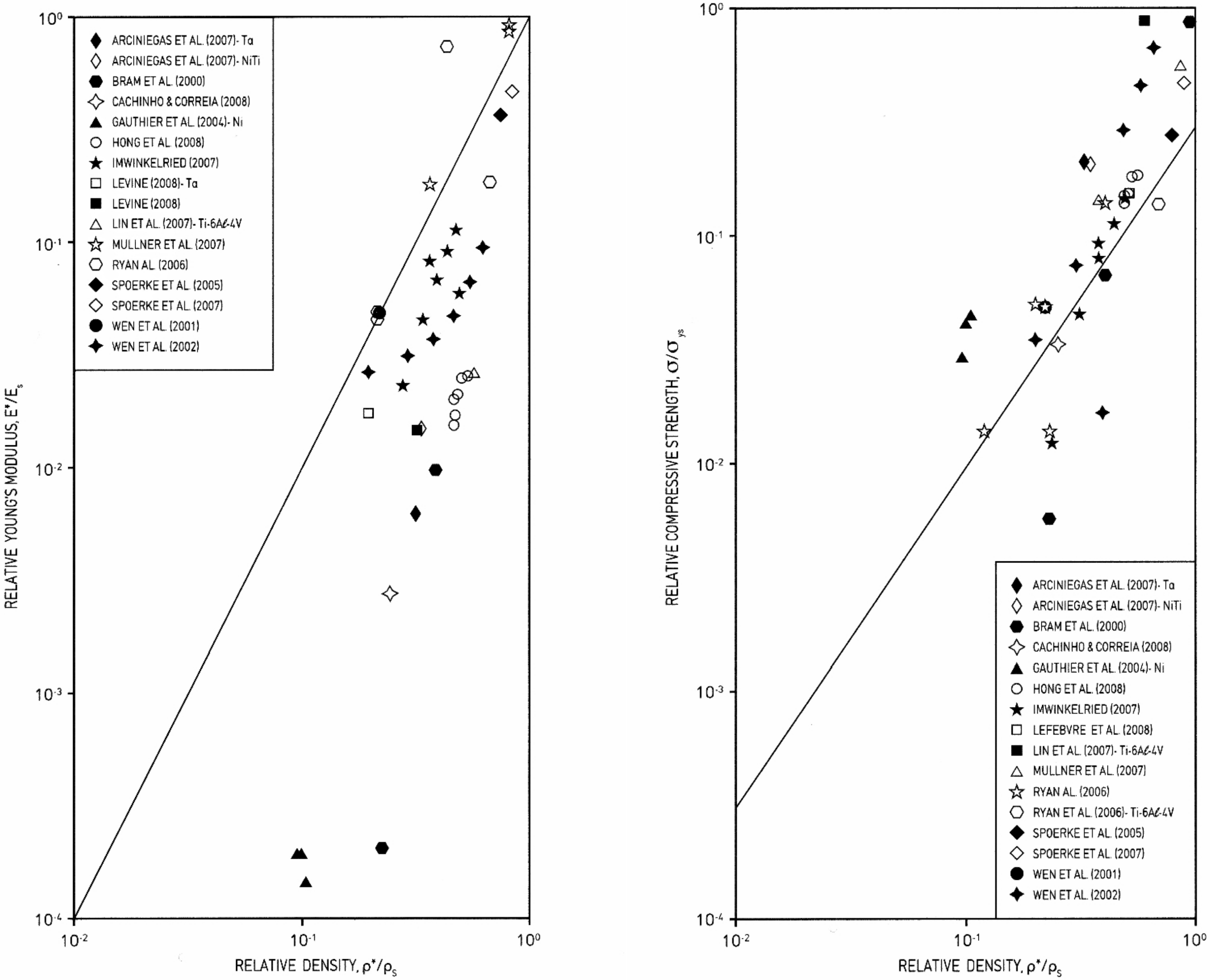

Gibson, L. J., M. Ashby, et al. *Cellular Materials in Nature and Medicine*. Cambridge University Press, © 2010. Figures courtesy of Lorna Gibson and Cambridge University Press.

Bone in Evolutionary Studies

Bone structure in evolutionary studies

- phylogenetic chart - big picture - structural biomaterials (mineralized)
- sponges - first multi celled animal
  - calcarea: $CaCO_3$ spicules (needles)
  - hexactinellida: SiO_2 - "glass sponges"
  - demospongiae: most sponges - some have SiO_2 spicules
    - spongin (type of collagen)

- cnidarians - eg. corals, jellyfish
  - corals $CaCO_3$
- Mollusca - bivalves, snails, octopus
  - if mineralized $CaCO_3$
- arthropods eg. hexapoda (insects), arachnide (spiders), crustaceans (shrimp, lobster)
  - exoskeleton of insects + spiders: chitin
  - crustaceans: chitin may be mineralized with $CaCO_3$

Vertebrates

- cyclostomata - jawless fish - lampreys hagfish
  - no vertebra - notochord
  - no bone
- Chondrichthyes - sharks, rays, skates
  - cartilaginous skeleton - some mineralization, but not true bone
- actinopterygii - ray finned fish
  - true bone
  - 450 million years ago (MYA)

Bone structure + loading

- bone grows in response to loading
- bone structure reflects mechanical loading + function e.g. quadruped vs ~~p~~ biped
- evolutionary studies have looked at trabecular bone architecture + density.

METAZOA

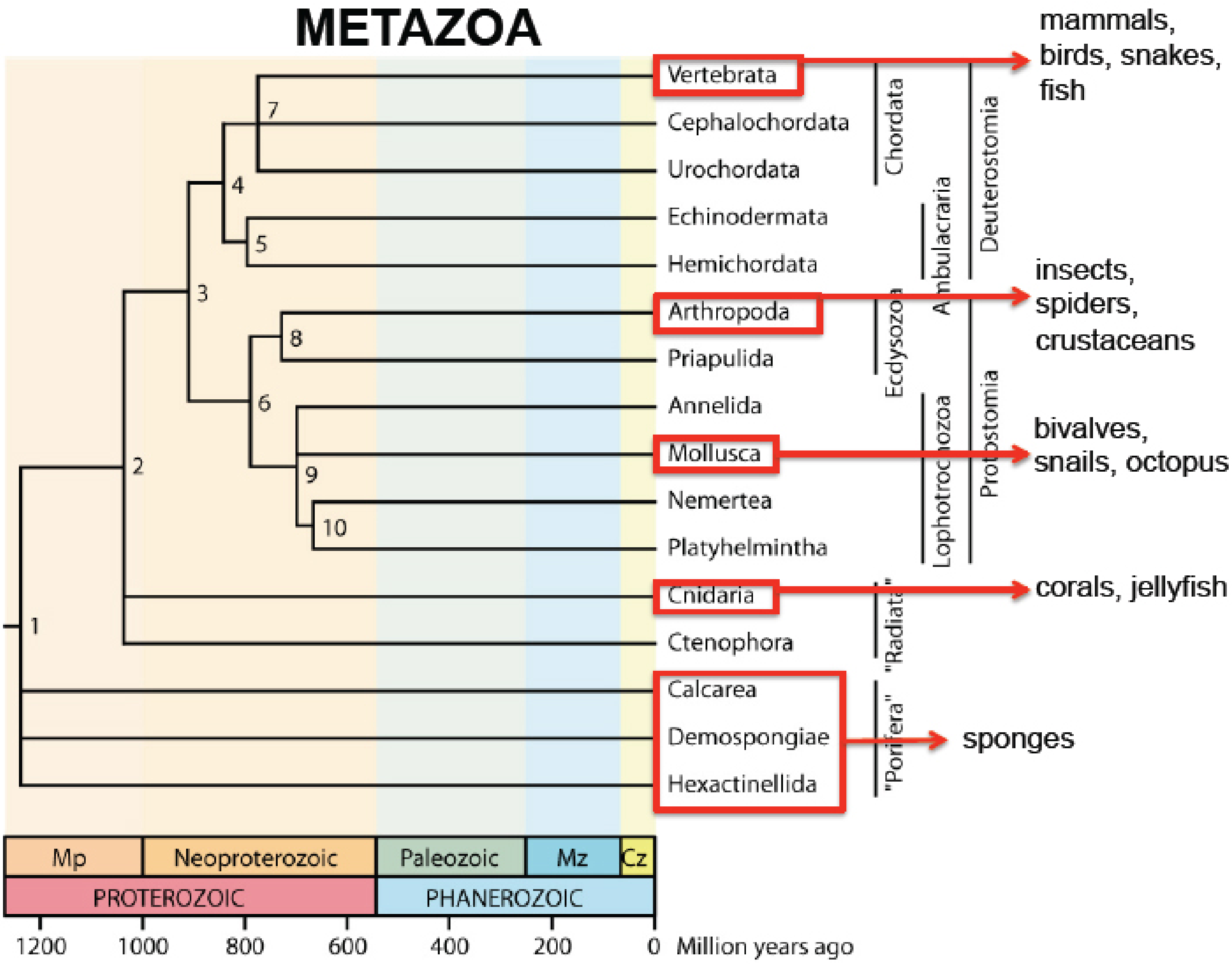

Fig. 2 A timetree of metazoan phyla. Divergence times are shown in Table 1. *Abbreviations*: Cz (Cenozoic), Mp (Mesoproterozoic), and Mz (Mesozoic).

Hedges and Kumar, 2009

Venus Flower Basket
(*Euplectella aspergillum*)

- Hierarchical structure
- Remarkably stiff, tough
- Joanna Aizenberg (Harvard)
- Aizenberg et al (2004) Biological glass fibers: correlation between optical and structural properties. PNAS

VERTEBRATA

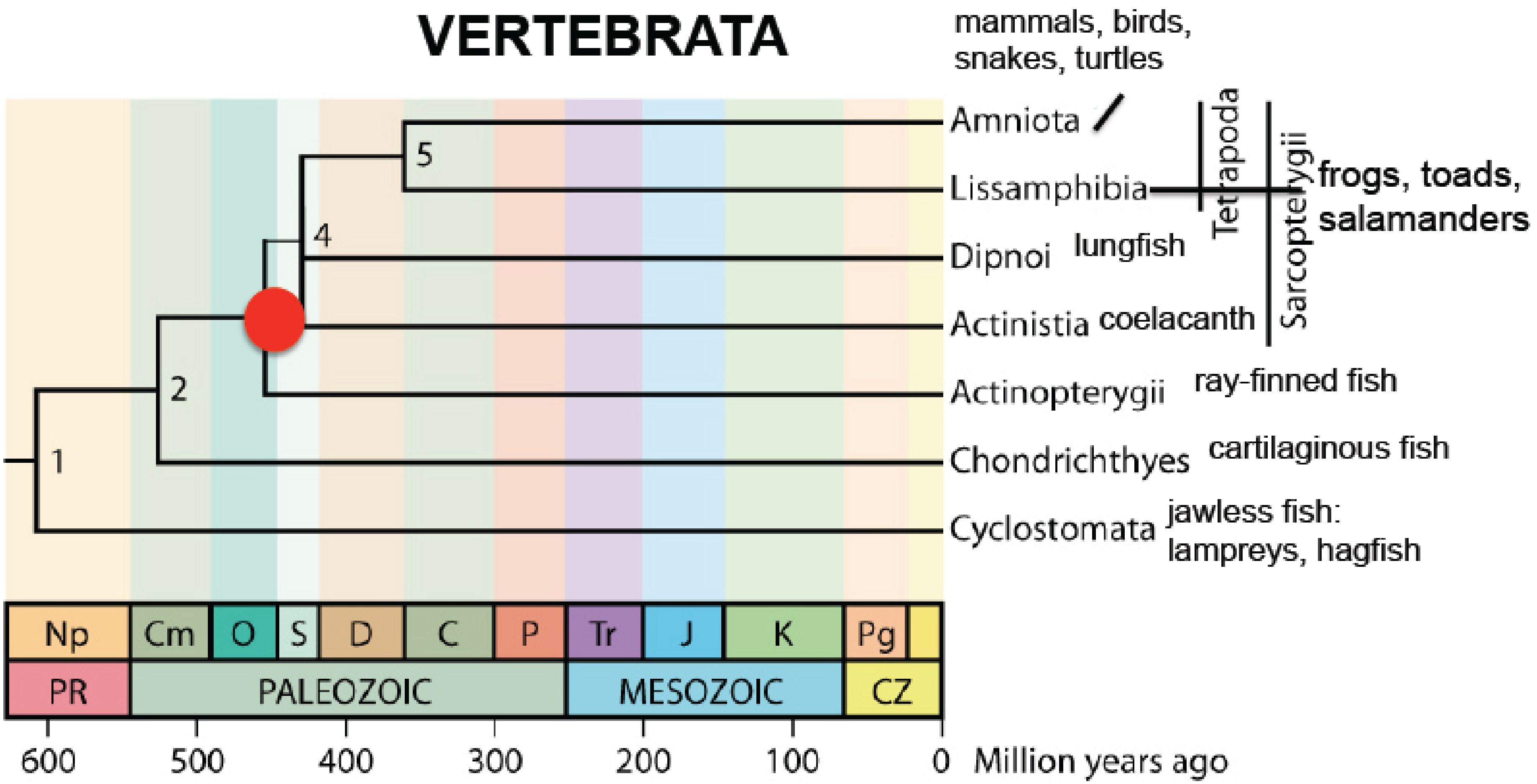

Fig. 2 A timetree of vertebrates. Times of divergence are averages of estimates from different studies listed in Table 1. *Abbreviations:* C (Carboniferous), Cm (Cambrian), CZ (Cenozoic), D (Devonian), J (Jurassic), K (Cretaceous), Np (Neoproterozoic), O (Ordovician), P (Permian), Pg (Paleogene), PR (Proterozoic), S (Silurian), and Tr (Triassic).

● Common ancestor of all boned vertebrates roughly 450 MYA

(Hagfish video)

Trabecular bone studies in human evolution

Oreopithecus bambolii (Rook et al, 1999)

- 7-9 MYA late Miocene hominid, found in Italy
- quadruped or biped?
- compared trabecular architecture in ilium in apes, O. bambolii, humans
- only had 2 fragments of ilium - left + right
- took radiographs of both + digitally reconstructed a single ilium

---

Comparisons

(a) posterosuperior margin - marginal handles thicker than apes

(b) anterosuperior margin - iib bundle relatively structured compared to apes

(c) anteroinferior margin - well developed a-i spine not seen in apes

(d) supra acetabular area - high density region

- Collectively, observations suggest O. bambolii trab. architecture in ilium more similar to humans than apes
- suggests habitual bipedal locomotion (humans - obligatory bipeds)

Oreopithecus bambolii: Ilium

Rook et al. (1999)

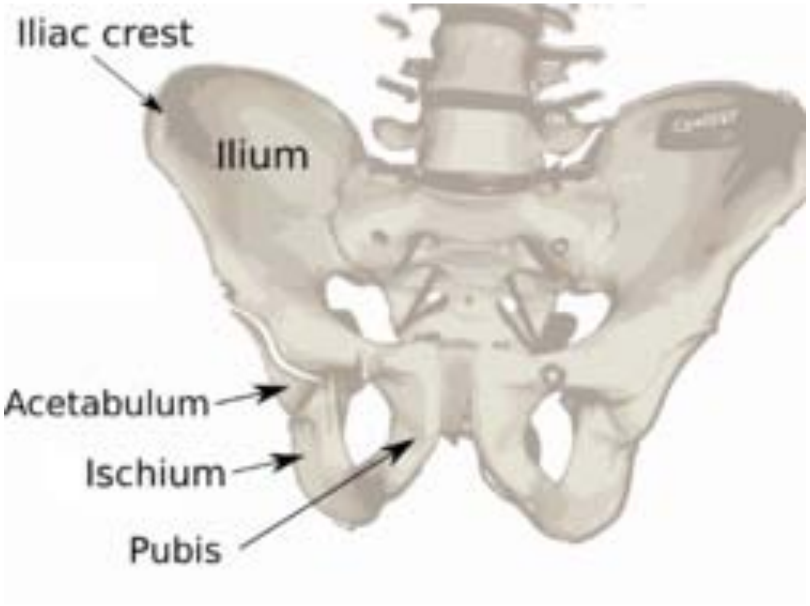

Image is in the public domain. Source: Wikimedia Commons.

http://en.wikipedia.org/wiki/Iliac_crest

Trabecular architecture: Ilium

Figure removed due to copyright restrictions. See Figure 1: Rook L., et al. "Oreopithecus was a Bipedal Ape after All." *Proceedings of the Natural Academy of Sciences* 96 (1999): 8795-99.

Digitally reconstructed ilium

Figure removed due to copyright restrictions. See Figure 2: Rook L., et al. "Oreopithecus was a Bipedal Ape after All." *Proceedings of the Natural Academy of Sciences 96* (1999): 8795-99.

Comparison of trabecular architecture

Figure removed due to copyright restrictions. See Figure 3: Rook L., et al. "Oreopithecus was a Bipedal Ape after All." *Proceedings of the Natural Academy of Sciences* 96 (1999): 8795-99.

3.054 / 3.36 Cellular Solids: Structure, Properties and Applications
Spring 2014